

FEM Applications of Catenary Type Structures

Viorel ANGHEL^{*1}, Stefan SOROHAN¹, Daniel HODOR²

*Corresponding author

¹“POLITEHNICA” University of Bucharest, Strength of Materials Department,
Splaiul Independentei 313, 060042, Bucharest, Romania,
vanghel10@gmail.com*, stefan.sorohan@upb.ro

²“SC Ventex Fire Protection SRL”,
Brasov, Romania,
proingex@gmail.com

DOI: 10.13111/2066-8201.2022.14.4.2

Received: 26 August 2022/ Accepted: 02 November 2022/ Published: December 2022

Copyright © 2022. Published by INCAS. This is an “open access” article under the CC BY-NC-ND license (<http://creativecommons.org/licenses/by-nc-nd/4.0/>)

Abstract: *The paper deals with Finite Element Modeling of catenary type structures starting from practical problems related to a single cable segment in the case of an electric transmission line. Finite element models allow the analysis of the resulting deformed position and stress state for a given configuration obtained by using the geometric and physical data of a cable. Beam type linear/nonlinear finite element models which can take into account also the temperature variation and extra loading on the cable were developed. Another application of this type of models is for the case of form finding of aerial refueling cable subjected to dynamic pressure. The results were obtained by the commercial finite element software ANSYS.*

Key Words: *Catenary, Single Cable Segment, Transmission Line, Aerial Refueling Cable, ANSYS*

1. INTRODUCTION

Generally, a cable is a structural member which withstands in tension only. Other denominations for this type of catenary structures are rope, wire rope, chain, string etc. A typical application for catenary based calculation is, for example, in the design of high voltage overhead line (OHL), [1]. When the lengths of the cables are smalls, one can use also the parabolic approximation of the catenary curve. Other applications as suspension bridges or cable cars, can present both geometric and material non-linear behavior. For this reason, in addition to analytical relations, the finite element modeling can be a powerful tool in such analysis, [2, 3]. For example in the reference [3] a special computer program based on an advanced cable element is presented for cable structures. It can take into account gravity, thermal and fluid drag effects. A more recent special academic software application for analysis of cable structures is described in [4].

For form finding and structural analysis of catenary structures other works use the available commercial finite element codes [5, 6]. After some analytical calculations this paper presents several applications by using the capabilities of the finite element code ANSYS. Different aspects of the applications concerning the electric transmission line analysis and for the form finding of an aerial refueling cable subjected to gravity and constant dynamic pressure are then discussed.

The catenary equation can be found in works like [1, 7]. A complete procedure to solve the equation of state can also be taken from [8]. Figure 1a presents the situation of a catenary with the ends in points A, B and vertex N. An arbitrary orthogonal coordinate system is used. The tension has a minimum value T_0 , and the maximum T value corresponds to point B. In this work, the catenary equation for preliminary calculations is used in the form:

$$y = y_0 + a \cdot \cosh\left(\frac{x - x_0}{a}\right), \quad (1)$$

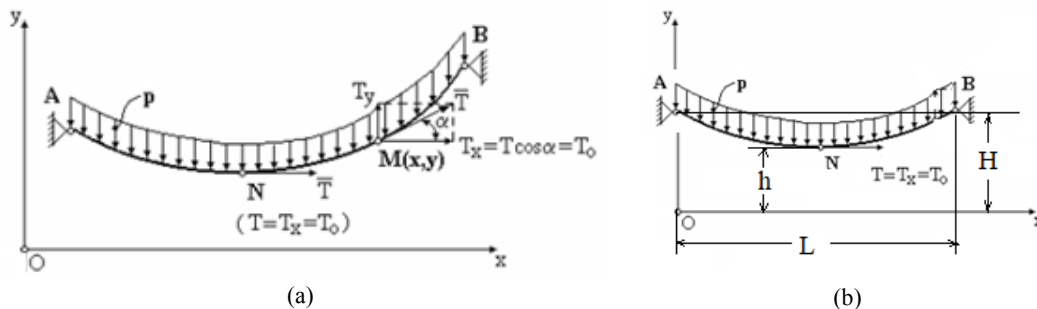


Fig. 1 – Catenary configurations

where the constants y_0 , x_0 and a are determined, imposing the followings conditions: points A and B are on the catenary curve and the total length of the catenary l_{AB} is prescribed.

One considers also a particular geometry with the following positions of points: A ($x_A = 0$, $y_A = H$) and B ($x_B = L$, $y_B = H$), thus with the supports at the same level (see figure 1b). Using this geometry one can obtain:

$$x_0 = \frac{L}{2}; \quad y_0 = H - a \cdot \cosh\left(\frac{L}{2a}\right). \quad (2)$$

In the literature many applications consider the origin of the coordinate system set at the vertex point N of the curve and in this manner the distance toward the left-hand or right-hand side support of the span is measured from the vertex, in both directions with a positive sign [9]. This is useful here, due to the symmetry, to obtain the parameter a imposing the condition:

$$l_{AB} = \int_{x_A}^{x_B} ds = 2 \int_0^{L/2} \cosh\left(\frac{x}{a}\right) dx = 2a \cdot \sinh\left(\frac{L}{2a}\right). \quad (3)$$

Then, the tensions in the cable are calculated with the following relations:

$$T = p \cdot (y - y_0); \quad T_0 = p \cdot a, \quad (4)$$

where $p = \rho Ag$ is the load due to gravity per unit length of the cable (ρ is the mass density, A is the cable cross-section area, $g = 9.81 \text{ m/s}^2$).

The minimum tension value is then T_0 and the maximum one is obtained for $y = y_{\max} = H$.

2. ANALYTICAL CALCULATIONS

A numerical example is presented here for the case $L = 40 \text{ m}$ and $H = 15 \text{ m}$. The material of the cable is steel having $\rho = 7850 \text{ kg/m}^3$ and circular cross-section area with the diameter $d = 50 \text{ mm}$.

One explores here the l_{AB} values between $L = 40 \text{ m}$ and the value corresponding to the ‘hanging cable’ (point N arrives on the Ox axis, [10]). Using the relations presented before, the idea is to calculate the a values in order to match the given lengths of the inextensible

cable. Some results are presented in Table 1. When the length of the cable tends to $L = 40$ m, the tension in the cable is increasing. It has a minimum value in the case of the hanging cable, here when $l_{AB} = 52.3$ m.

Table 1. Results of analytical calculations

l_{AB} [m]	a [m]	$y_{min} = h$ [m]	T_0 [N]	$\sigma_0 = T_0/A$ [MPa]	$\sigma_{max} = T/A$ [MPa]
40.1	162.78	13.77	24613.97	12.53	12.63
40.5	73.13	12.25	11058.40	5.63	5.84
42	36.77	9.43	5560.50	2.83	3.26
45	23.51	5.97	3554.75	1.81	2.51
48	18.77	3.30	2839.23	1.44	2.35
50	16.91	1.72	2556.33	1.30	2.32
52	15.53	0.24	2348.69	1.19	2.33
52.3	15.36	0.03	2322.01	1.18	2.34

3. FINITE ELEMENT MODEL FOR SUSPENDED CATENARY

For a case considered before with a cable manufactured on steel (Young’s modulus $E = 2e11$ Pa; mass density $\rho = 7850$ kg/m³) having the cross-section diameter $d = 50$ mm and the initial undeformed length $l_{AB} = 42$ m, one calculates the equilibrium position using a finite element model in ANSYS Classic.

One end of the cable is pinned and the other is free on horizontal direction (simply supported on vertical).

Both ends are on the same vertical height $H = 15$ m and the horizontal tension force at the free end is considered $F_0 = T_0 = 5560.5$ N. The created APDL command code can consider the effect of temperature variation and supplementary loads (hail, wind).

For this example, these additional effects are neglected. The model is kept 2D and uses BEAM188/189 elements. To eliminate the bending effects, the section of the cable is considered an equivalent very thin rectangle having the same cross section area ($A = bh = \pi d^2/4$). The model is nonlinear.

The initial position of the cable is horizontal, then, under the tension and gravity loads, the cable moves toward the equilibrium position. Figure 2 shows the final position and vertical displacements of the cable. The maximum vertical displacement value is 5.573 m and corresponds to $h = y_{min} = 15 - 5.573 = 9.427$ m (9.43 m in the analytical calculation).

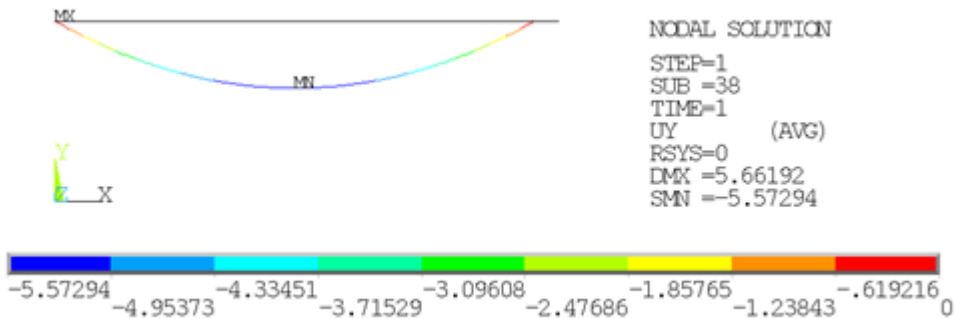


Fig. 2 – Final position and vertical displacements UY of cable, [m]

The maximum horizontal displacement is 1.999 m, (see Fig. 3) and corresponds to the distance between the two pillars $L = l_{AB} - 1.999$ m = 40 m, used in the analytical calculations.

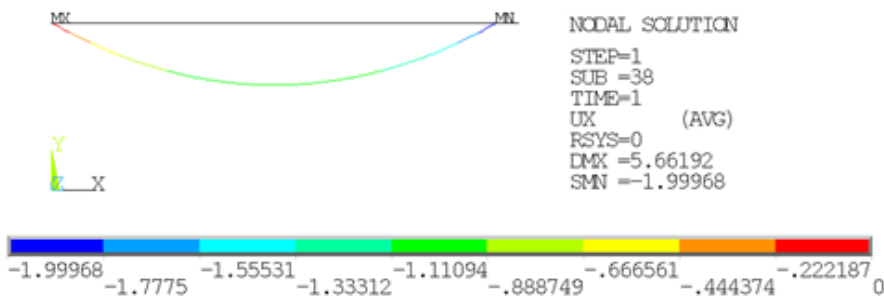


Fig. 3 – Final position and horizontal displacements UX of cable, [m]

Figure 4 shows the axial tension values. The maximum value corresponds to an average maximum axial stress $\sigma_{max} = T/A = 6403.23/1963.5 = 3.26$ MPa just as in Table 1.

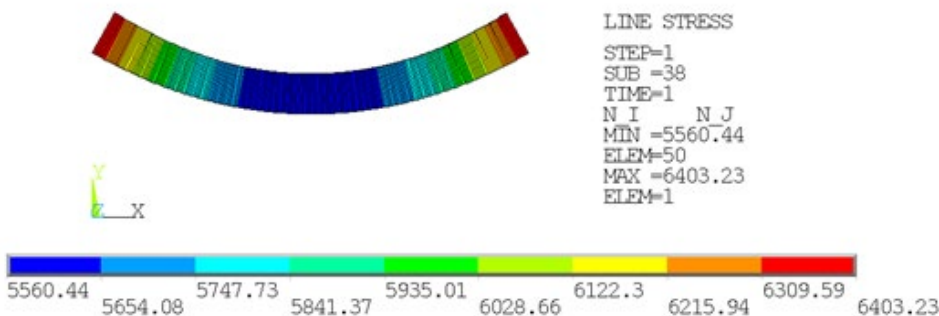


Fig. 4 – Axial tension in the cable [N]

In figure 5 one can see the reactions in the two supports. The vertical reactions are in equilibrium with the total weight of the cable ($2 \times 3175.33 \text{ N} = \rho g l_{AB}$), the horizontal reaction value in a support is $T_0 = F_0 = 5560.52 \text{ N}$ and the total reactions are the maximum tensions loads located at supports:

$$T = \sqrt{5560.52^2 + 3175.33^2} = 6403.28 \text{ N}$$

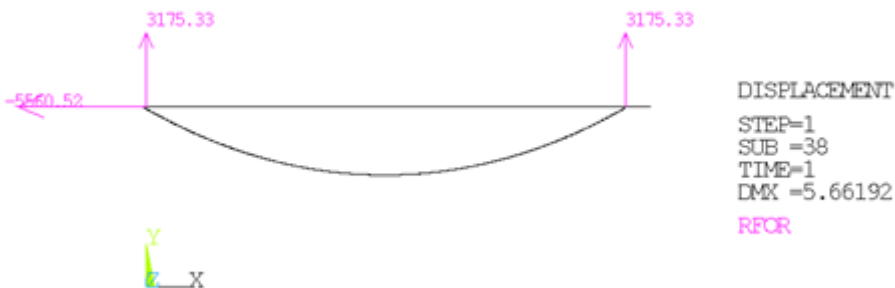


Fig. 5 – Reactions in the supports [N]

In this case, the calculated values by FEM are in agreement with the analytical results. However, although the cable should only be subjected to stretching, small values of shear forces (maximum 19.46 N) and bending moments (maximum 5.56 Nm) are obtained as residues. This is a measure of the accuracy of the model.

4. FINITE ELEMENT MODEL OF AN AERIAL REFUELING CABLE

Generally, in the case of an aerial cable towed system, the distributed forces to be considered are the gravity, the aerodynamic forces, and some other forces due to the added mass of air surrounding the cable. There is also a special component at the free end (figure 6).

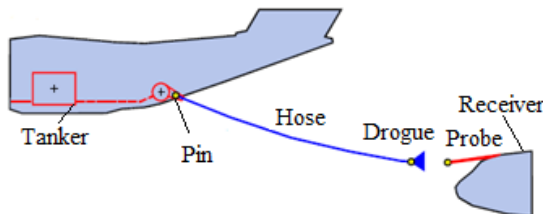


Fig. 6 – Aerial refueling scheme

The problem of the study of an aerial refueling cable is addressed in works like [11-14]. For example in [12] the kinematics equation is solved using the fourth-order Runge–Kutta method and [13] uses a model with links and lumped masses in order to find the steady state position of the hose-drogue. In [14] a generalized model for this problem is analyzed by the FEM. The hose is modeled by curved beam elements and the towed body is considered as a lumped mass. In this paper some numerical examples are presented using a 2D FE model and data adapted from [12]. The cable is actually a hose having annular cross-section (external diameter $D = 67.3$ mm; internal diameter $d = 50.8$ mm) and a fixed length $L = 14.33$ m. The initial position is considered straight at rest, horizontal, vertical or inclined. It is considered pinned at the upper end (hose attachment point on the tanker) and has a suspended rigid mass at the drogue attachment point ($M_c = 29.5$ kg at the bottom end). It was neglected the fluid inside (empty hose). The material of the hose is considered homogeneous and isotropic with $E = 6$ GPa, $\nu = 0.3$ and $\rho = 2633.2$ kg/m³ (the hose has the mass per unit length 4.09 kg/m). The material is considered to have a linear behavior but the finite element model is nonlinear as large deflections are taken into account.

There are three different situations in which an attempt is made to achieve the equilibrium position of the suspended cable (hose) with one end attached to an aircraft (tanker):

a) the aircraft has a given horizontal acceleration and the aerodynamic forces are neglected ($a_x = a_y = g = 9.81$ m/s² (for a partial model validation);

b) the aircraft has a constant velocity and one considers arbitrary constant aerodynamic distributed forces on the cable ($a_x = 0$ and normal/tangential components of the distributed forces are $p_n = 50$ N/m and $p_t = 25$ N/m respectively). A horizontal constant aerodynamic force $F_0 = 500$ N is considered in the suspended mass;

c) the aircraft has a lower constant velocity and one considers arbitrary constant aerodynamic distributed forces on the cable ($a_x = 0$ and normal/tangential components of the distributed forces are $p_n = 10$ N/m and $p_t = 0$ N/m, respectively). A constant horizontal aerodynamic force $F_0 = 500$ N is also considered in the suspended mass.

The most difficult problem is how to apply the distributed pressure on the cable due to the incoming airflow at a given speed that depends on the current (unknown) position of the finite element (hose segment). For this reason, here (at this stage) only constant normal and tangential components of the distributed aerodynamic forces are applied on the cable (constant values on all cable elements). The following results are obtained with the total length of the cable discretised in 50 finite elements of BEAM type [15]. The distributed pressure loads are applied using SURF 157 elements. Figure 7 shows the final position of the cable in case a) when the initial position of the cable is horizontal.

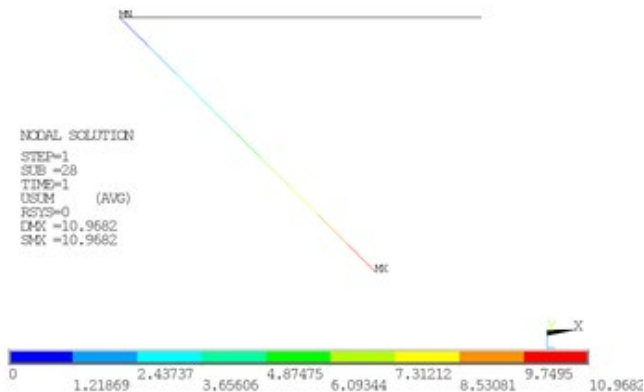


Fig. 7 – Total displacements [m] and initial (horizontal)/final positions of cable (case a)

Figure 8 shows the final position of the cable in case a) when the initial position of the cable is vertical.

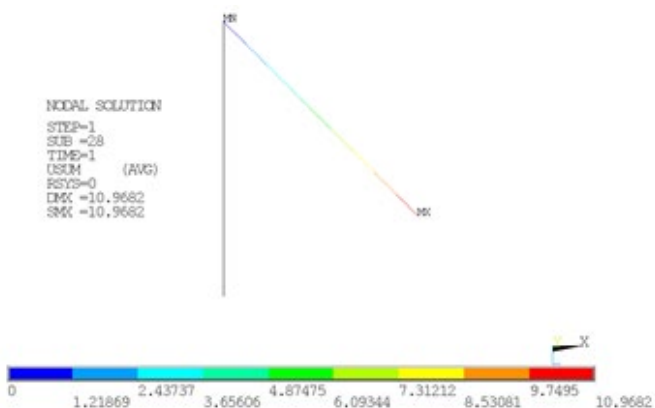


Fig. 8 – Total displacements [m] and initial (vertical)/final positions of cable (case a)

Figure 9 shows the final position of the cable in case a) when the initial position of the cable is inclined at 45°.

In this case the initial position is the same with the final one, so the obtained displacements are very small.

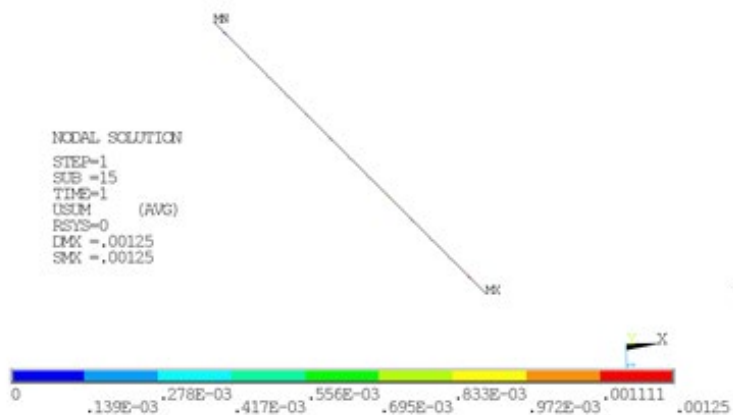


Fig. 9 – Total displacements [m] and initial (inclined)/final positions of cable (case a)

Figure 10 shows the axial force and the reactions for the final position for all these three applications.

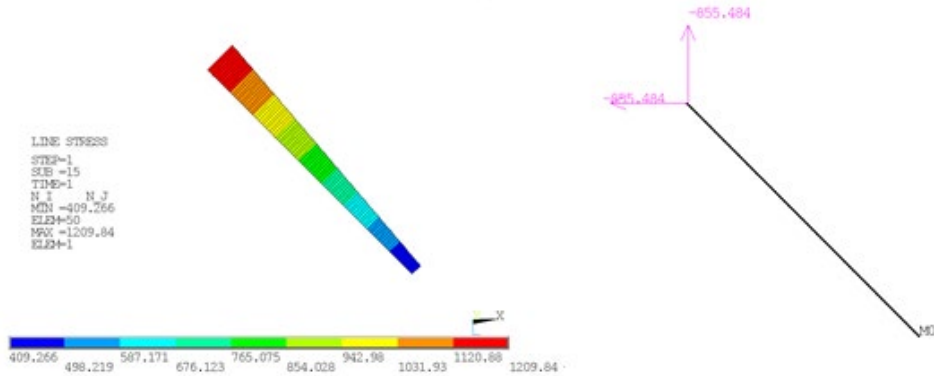


Fig. 10 – Axial force and reactions at the pin in the final position of cable [N] (case a)

So, regardless of the starting position of the cable, the final equilibrium position is the same. The convergence is faster, when the initial position of the cable is very close to the final one (inclined cable). The calculations performed in case a) represent a partial validation of such a model.

Figure 11 shows the final position of the cable in case b) when the initial position of the cable is horizontal.

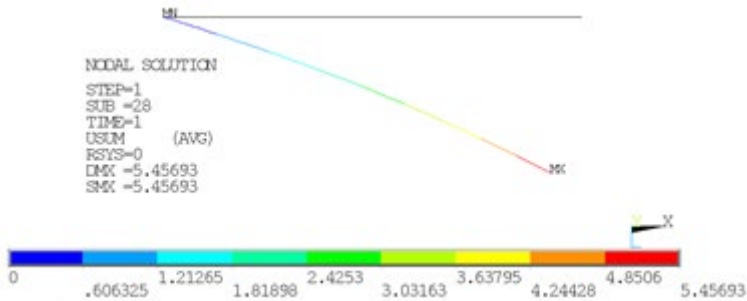


Fig. 11 – Total displacements [m] and initial (horizontal)/final positions of cable (case b)

Figure 12 shows the final position of the cable in case b) when the initial position of the cable is vertical.

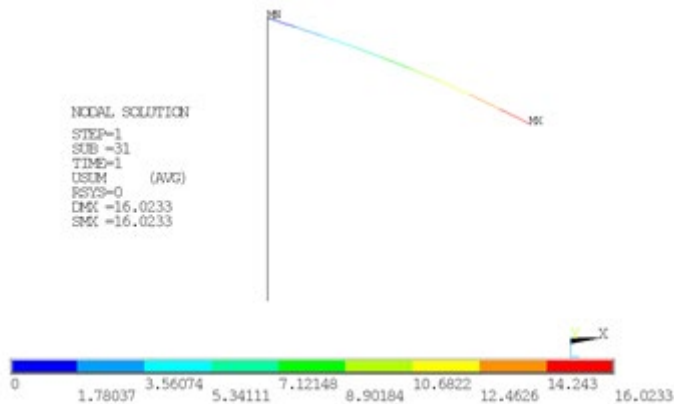


Fig. 12 – Total displacements [m] and initial (vertical)/final positions of cable (case b)

Figure 13 shows the final position of the cable in case b) when the initial position of the cable is inclined.

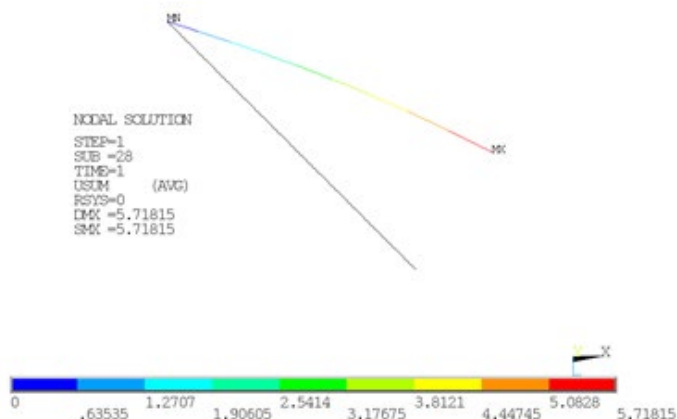


Fig. 13 – Total displacements [m] and initial (inclined)/final positions of cable (case b)

Figure 14 shows the axial force and the reactions for the final position (case b).

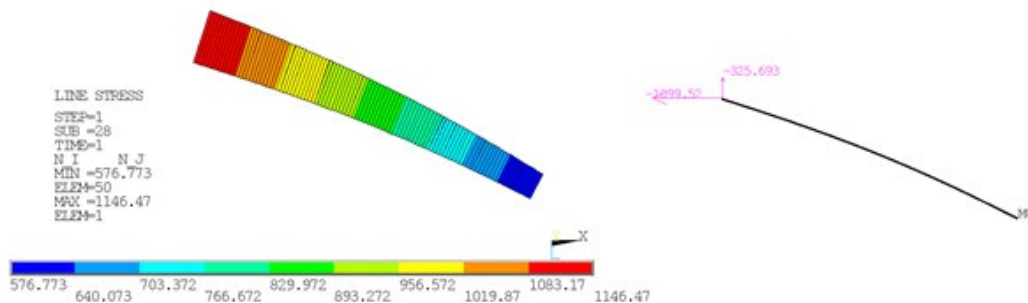


Fig. 14 – Axial force and reactions at the pin in the final position of cable [N] (case b)

The final equilibrium position is the same in all three variants of case b). Figure 15 shows the final position of the cable in case c) when the initial position of the cable is horizontal. As it was established before, in this case the constant dynamic pressure is lower than in case b).

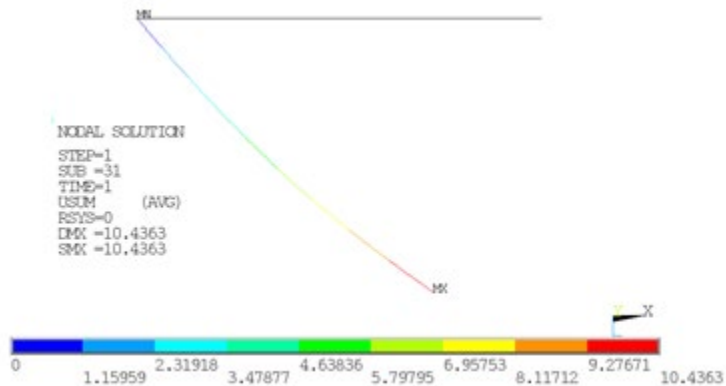


Fig. 15 – Total displacements [m] and initial (horizontal)/final positions of cable (case c)

Figure 16 shows the final position of the cable in case c) when the initial position of the cable is vertical.

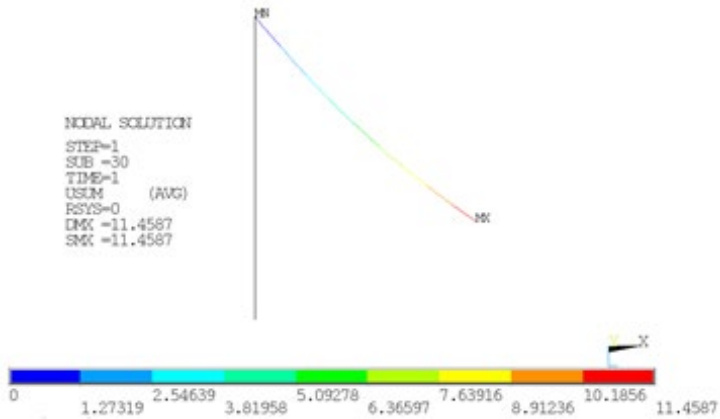


Fig. 16 – Total displacements [m] and initial (vertical)/final positions of cable (case c)

Figure 17 shows the final position of the cable in case c) when the initial position of the cable is inclined.

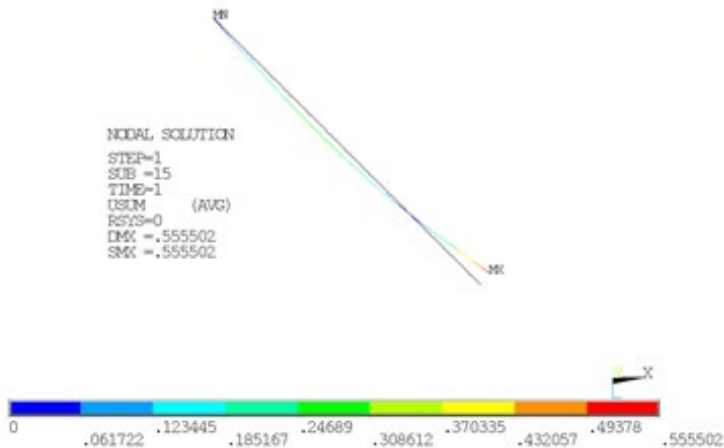


Fig. 17 – Total displacements [m] and initial (inclined)/final positions of cable (case c)

Figure 18 shows the axial force and the reactions for the final position (case c).

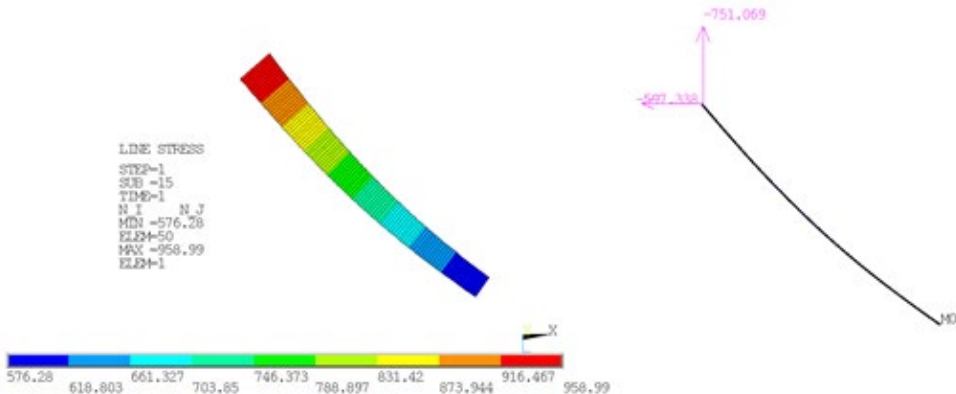


Fig. 18 – Axial force and reactions at the pin in the final position of cable [N] (case c)

The final equilibrium position is the same in all three variants of case c).

5. CONCLUSIONS

This paper presents some FE models for the analysis of catenary type structures. Two types of usual configurations are considered namely suspended (pinned cables at both ends) and cables pinned at one end and free at the other one. The first case is typical for the design of high voltage overhead lines (OHL), while the other can represent the case of an aerial refueling cable in aerospace applications. The nonlinear models use BEAM type elements in ANSYS Classic APDL. The material of the cable works in elastic range while large deflections are considered. The results of the model for the first configuration were compared to the analytical solution available from literature. In the case of the aerial refueling cable, the equilibrium position is obtained for a prescribed dynamic pressure (uniform distributed forces) and gravity acting in the same plane. The convergence of the nonlinear process is better when the starting position is close to the final one. Further improvement of the model consists in the appropriate description of the non-uniform aerodynamic drag forces which depend on the local inclination angle. The models presented further demonstrate the possibility of using the formidable capabilities of ANSYS software in such nonlinear analyses.

ACKNOWLEDGEMENT

This article is an extension of the paper presented at *The International Conference of Aerospace Sciences, "AEROSPATIAL 2022"*, 13 – 14 October 2022, Bucharest, Romania, *Hybrid Conference*, Section 4 – Materials and Structures.

REFERENCES

- [1] D. A. Douglass, R. Thrash, *Sag and Tension of Conductor*, Taylor & Francis Group LLC., 2006.
- [2] H. B. Jayaraman, W. C. Knudson, A curved element for the analysis of cable structures, *Computers & Structures*, Vol. **14**, No. 3–4, pp. 325-333, 1981.
- [3] A. H. Peyrot, A. M. Goulois, Analysis of cable structures, *Computers & Structures*, Vol. **10** (5), pp. 805-813, 1979.
- [4] R. S. Costa, A. C. C. Lavall, R. G. Lanna da Silva, A. P. dos Santos, H. F. Viana, Cable structures: An exact geometric analysis using catenary curve and considering the material nonlinearity and temperature effect, *Engineering Structures*, Vol. **253**, Article 113738, 2022.
- [5] E. Madenci, I. Güven, *The finite element method and applications in engineering using ANSYS*, Springer, 2015.
- [6] L. Liao, B. Du, Finite Element Analysis of Cable-Truss-Structures, *51st AIAA/ASME/ASCE/AHS/ASC Structures, Structural Dynamic and Materials Conference*, 12-15 April, Orlando, Florida, 2010.
- [7] R. Voinea, D. Voiculescu, V. Ceaușu, *Mechanics* (in Romanian), Ed. Didactică și Pedagogică, Bucharest, 1975.
- [8] G. A. Costello, *Theory of wire rope*, Springer, 1987.
- [9] A. Hatibovic, Derivation of Equations for Conductor and Sag Curves of an Overhead Line Based on a Given Catenary Constant, *Periodica Polytechnica, Electrical Engineering and Computer Science*, Vol. **58** (1), pp. 23–27, 2014.
- [10] N. Chatterjee, B. G. Nita, The hanging cable problem for practical applications, *Atlantic Electronic Journal of Mathematics*, Vol. **4**(1), pp. 70-77, 2010.
- [11] N. Fezans, T. Jann, Modeling and Simulation for the Automation of Aerial Refueling of Military Transport Aircraft with the Probe-and-Drogue System, *AIAA AVIATION Forum, Denver, Colorado, AIAA Modeling and Simulation Technologies Conference*, 5-9 June 2017.
- [12] J. Cheng, K. Ji, Dynamic modeling and simulation of variable-length hose-drogue aerial refueling systems, *AIP Advances*, Vol. **12**, 015104, 2022.
- [13] K. Ro, J. W. Kamman, Modeling and simulation of hose-paradrogue aerial refueling systems, *J. Guid., Control, Dyn.*, Vol. **33**(1), pp. 53–63, 2010.
- [14] Z. H. Zhu, S. A. Meguid, Modeling and simulation of aerial refueling by finite element method, *International Journal of Solids and Structures*, Vol. **44**, pp. 8057–8073, 2007.
- [15] * * * *Mechanical APDL (ANSYS)*, Version 21.1 Academic Teaching Advanced Utility Menu, 2006.